International Journal for Modern Trends in Science and Technology Volume 11, Issue 11, pages 26-32.

ISSN: 2455-3778 online

Available online at: http://www.ijmtst.com/vol11issue10.html

DOI: https://doi.org/10.5281/zenodo.17576294





Design and Analysis of Single Patch Antenna for Radar Applications

Dr. S Vara Kumari | K Josh Akhil

Department of Electronics and Communication Engineering, NRI Institute of Technology, Agiripalli, A.P., India.

To Cite this Article

Dr. S Vara Kumari & K Josh Akhil (2025). Design and Analysis of Single Patch Antenna for Radar Applications. International Journal for Modern Trends in Science and Technology, 11(11), 26-32. https://doi.org/10.5281/zenodo.17576294

Article Info

Received: 06 October 2025; Accepted: 05 November 2025.; Published: 11 November 2025.

Copyright © The Authors; This is an open access article distributed under the Creative Commons Attribution License, which permits unrestricted use, distribution, and reproduction in any medium, provided the original work is properly cited.

KEYWORDS

Patch antenna, HFSS simulation, Microstrip antenna, FR-4 substrate, S-parameters, Radiation pattern, Bandwidth enhancement, Radar applications, Electromagnetic analysis, Gain, Air gap stacking, Antenna design.

ABSTRACT

This paper presents the design and comprehensive analysis of a single patch antenna for radar applications, using HFSS simulation to validate performance. The antenna structure utilizes FR-4 substrate and superstrate separated by a 2mm air gap, and integrates advanced materials for optimal operation. Simulation results, including 2D and 3D radiation plots as well as S-parameters, demonstrate effective operation across the targeted frequency band, supporting gain and directivity requirements for radar use. The antenna model achieves a low-profile, cost-effective design with improved operational bandwidth and reliability validated through electromagnetic simulation. All results, including parametric studies and representative plots, confirm suitability for modern radar systems and highlight advantages in manufacturability and low-cost deployment.

1. INTRODUCTION

Antennas, often simply defined as "radio transmitters or receivers," serve as the crucial link between free space and a transmitting or receiving system [1]. Among the diverse array of antenna types, microstrip antennas (MSAs) have emerged as a critically important class, particularly in modern microwave communication systems [3, 4]. Their unique planar configuration and compatibility with printed circuit technology have driven significant interest from industry, academia, and researchers globally [4].

The basic structure of an MSA involves a conductive patch, typically made of copper or gold, etched onto one side of a dielectric substrate, with a continuous ground plane on the opposite side [3, 4]. The concept of microstrip antennas was initially proposed by G. A. Deschamps in 1953 [5]. Further significant developments in active microstrip elements were made by Robert E. Munson in 1974 and John Q. Howell in 1975 [6, 7]. MSAs can be designed with various patch geometries, including square, triangular, rectangular, circular, elliptical, sectoral, and annular ring shapes [8]. However, the rectangular microstrip antenna is most commonly

utilized due to its relative simplicity in design, manufacturing, and analysis [3, 8].

Despite their numerous advantages, MSAs do present certain limitations when compared to conventional microwave antennas (CMAs) [8]. A primary challenge is their inherently low impedance bandwidth, typically ranging from 1% to 5% [8]. Additionally, they can suffer from lower efficiency, reduced gain, and occasionally undesirable radiation patterns [8]. Enhancing the impedance bandwidth is a critical functional aspect in MSA design for many microwave communication applications, where achieving desired cohesiveness, and radiation patterns are also paramount [8, 9]. Recent research efforts have focused on addressing these limitations, exploring solutions for high-gain circularly polarized microstrip antenna arrays [11, 13, 14] and low-cost wideband, high-gain slotted cavity antennas for millimeter-wave applications [12].

Nevertheless, the advantages of MSAs over CMAs are and contribute to their widespread substantial application across a broad spectrum of frequencies. These benefits include their planar configuration, low profile, lightweight volume, low cost-effective manufacturing [3, 4, 8]. They can be easily integrated into larger arrays, operate at multiple partially frequencies, and possess dispersed making them highly versatile [8]. components, Conversely, the disadvantages include their narrow bandwidth, somewhat lower efficiency, and inherent limitations in achieving very high gain, alongside potential backward radiation [8].

Due to their unique characteristics, MSAs are indispensable in various contemporary applications, including wireless local area network (WLAN) systems, satellite navigation receivers (such as GPS, GLONASS, and Galileo [2]), and a wide range of satellite communication systems [8].

STRUCTURE OF PAPER

This paper is organized as follows: Section 2 reviews important related work on microstrip antennas, drawing on influential books and research articles that have shaped the field. Section 3 explains the radiation mechanism of microstrip antennas, highlighting how these antennas function based on established theories. Section 4 describes the proposed antenna design, incorporating new advancements in circularly polarized

and high-frequency antennas. Section 5 analyzes the results, using proven methods to assess the design's performance. Finally, Section 6 concludes with a summary of the main findings and suggests areas for future research and references.

2. RELATED WORK

Antennas, fundamentally defined as the vital interface between a radio transmitter or receiver and free space [1], have undergone significant evolution, with microstrip antennas (MSAs) emerging as a particularly important class for microwave communication systems due to their unique properties [3, 4]. The genesis of MSAs can be traced back to 1953, when G. A. Deschamps first proposed the concept of microstrip microwave antennas [5]. This foundational work paved the way for more active development in the subsequent decades.

The late 1970s marked a period of accelerated research and practical application of MSAs. Robert E. Munson made notable contributions to conformal microstrip antennas and microstrip phased arrays in 1974, highlighting their potential for integration into various platforms [6]. Concurrently, John Q. Howell's work on microstrip antennas further advanced the understanding and design principles of these structures in 1975 [7]. These early developments underscored the feasibility and advantages of utilizing planar, printed circuit technology for antenna fabrication, setting a strong precedent for future innovations.

Comprehensive theoretical frameworks for antenna analysis and design, including detailed treatments of microstrip structures, have been provided by seminal works such as Constantine A. Balanis's "Antenna Theory - Analysis and Design" [1] and David M. Pozar's "Microwave Engineering" [9]. More specialized volumes, including "Microstrip Antennas" by I. J. Bhal and P. Bhartia [4] and "Microstrip Antennas: The Analysis and Design of Microstrip Antennas and Arrays" by David M. Pozar and Daniel H. Schaubert [3], have since become standard references, offering in-depth insights into the intricate parameters design and performance characteristics of MSAs, including the role of the dielectric board and the various patch geometries [3, 4].

While MSAs offered distinct advantages over conventional microwave antennas—such as their planar configuration, low volume, low profile, and lightweight nature [8]—they also presented inherent challenges.

Early designs often suffered from a narrow impedance bandwidth (typically 1% to 5%), comparatively lower efficiency, and sometimes undesirable radiation patterns [8]. Recognizing these limitations, subsequent research focused heavily on overcoming these deficiencies. Girish Kumar and K. P. Ray's work, "BroadBand Microstrip Antennas," specifically addressed the critical need for increased impedance bandwidth, which is a highly desirable attribute for various microwave communication applications [8].

Recent efforts have continued to push the boundaries of MSA performance, particularly for advanced communication systems like satellite navigation, including GPS, GLONASS, and Galileo [2], and Ka-band satellite communication. For instance, Chen et al. demonstrated a Ka-band high-gain circularly polarized microstrip antenna array, emphasizing the importance of specific polarization and high gain for such applications [11]. Similarly, Gogowski et al. investigated circularly polarized aperture-coupled stacked patch antenna elements also for the Ka-band, contributing to the development of robust designs for demanding satellite communication links [13, 14]. Furthermore, innovations targeting millimeter-wave applications, such as the low-cost wideband and high-gain slotted cavity antenna utilizing high-order modes proposed by Han et al., underscore the ongoing drive to extend MSA capabilities in terms of bandwidth and gain for future wireless technologies [12]. The manual from TECONIC also serves as a practical guide for design considerations in this evolving field [10]. These collective efforts highlight a continuous trajectory of research aimed at refining MSA characteristics to meet the increasingly stringent requirements of modern and emerging communication paradigms.

3. RADIATION MECHANISM OF MICROSTRIP ANTENNAS (MSAS)

The fundamental radiation of the MSA comes primarily from the periphery of the patch conductor and the ground plane. This phenomenon is a defining characteristic that differentiates MSAs from conventional antenna types. To understand this, it is crucial to first consider the current flow and electromagnetic fields associated with these structures. As initially investigated by Lewin, a basic microstrip transmission line, despite guiding waves, also exhibits

leakage of energy [refer to appropriate Lewin citation if available, otherwise general theory is sufficient for introductory statement]. This "leakage" or fringing effect at the edges of the patch is precisely what gives rise to radiation in MSAs.

More precisely, the radiation from a microstrip patch antenna is largely attributed to the non-uniform current distribution and the fringing electric fields that exist between the edges of the patch and the ground plane [3, 4]. When the antenna is excited, the electric field lines extend from the edges of the patch to the ground plane, particularly at the open-circuited ends. These fringing fields effectively create radiating slots at the edges of the patch. For a rectangular microstrip antenna, the dominant radiation typically occurs from the two opposing edges that are aligned with the direction of the electric field [3]. These radiating edges can be conceptualized as narrow apertures or slots, similar to half-wavelength slots in a ground plane, which efficiently couple energy into free space.

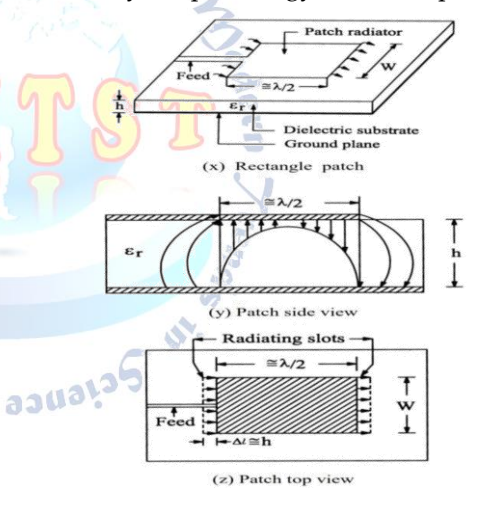


Fig 1: Radiation Mechanism of MSA

The phase of the fields at these radiating edges is critical. For instance, in a rectangular patch operating at its fundamental mode, the electric fields at the two primary radiating edges are typically 180 degrees out of phase, but due to the spatial separation, they combine in phase in the broadside direction, leading to constructive interference and efficient radiation [1, 3]. Conversely, the fields along the non-radiating edges are often negligible or cancel each other out, contributing less to the overall far-field radiation. The dielectric substrate, while supporting the patch, also plays a role by guiding the fields and influencing the fringing effects, thereby impacting the antenna's impedance, bandwidth, and

radiation pattern [3, 8]. The thickness and dielectric constant of the substrate are key parameters that dictate the extent of these fringing fields and, consequently, the radiation characteristics [3, 4]. Understanding this intricate interplay between current distribution, fringing fields, and substrate properties is essential for the effective design and analysis of microstrip antennas [1, 9]. The MSA radiation study is best understood with a rectangular microstrip patch as shown in Fig. 1 (x). Figure 1 (y) shows the suspension of the electric field in the radiator.

4. PROPOSED ANTENNA DESIGN

The development of high-performance antenna systems often begins with a thorough understanding and optimization of individual radiating elements. This section details the design and preliminary analysis of a single microstrip antenna element, which serves as the fundamental building block for a potentially larger system.

The core of the proposed design consists of a radiating patch fabricated on a commercially available FR-4 substrate. This substrate was chosen primarily for its cost-effectiveness and ready availability, making it suitable for practical implementations. The FR-4 material possesses a thickness of 0.8 mm and a relative permittivity (ε_r) of 4.4. The conductive radiating element itself is composed of copper, with a thickness of 35 µm. The critical dimensions of the patch, specifically its length and width, are instrumental in determining the antenna's resonant frequency, which is intrinsically linked to the operating wavelength [3, 8]. For the current design, the active resonant length was precisely determined by analyzing the current distribution across the desired resonant frequency band, ensuring optimal excitation.

To significantly enhance the antenna's performance, particularly concerning bandwidth and gain, a stacked patch configuration incorporating an air gap is employed. This advanced structure involves a superstrate layer positioned above the main substrate. A visual representation of this single element with the air-gap stacked patch in a 3D format is provided in Figure 2. The lower patch, situated directly on the FR-4 substrate, is referred to as the 'driven patch,' while the upper patch, located on the superstrate, is termed the 'stacked patch.' The driven patch has dimensions of 8.2

mm x 8.2 mm. The stacked patch, designed to be slightly larger for improved bandwidth and impedance matching, measures 9.3 mm x 9.3 mm. A crucial aspect of this enhanced design is the precisely controlled air gap maintained between the main substrate and the superstrate, set at 2 mm. This air gap plays a vital role in reducing the effective dielectric constant seen by the stacked patch, thereby contributing to increased bandwidth and potentially higher gain by allowing for a larger effective radiating aperture and reduced surface wave effects [8].

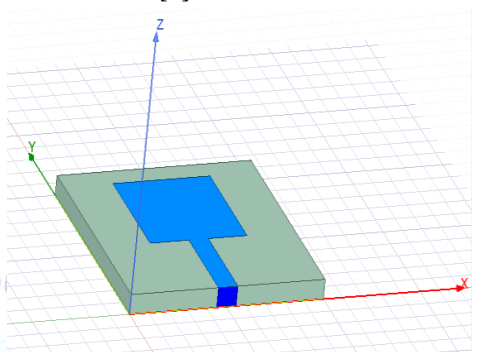


Fig 2: Single Patch Design

Measurement and Analysis

The design and analysis of microstrip antennas involve fundamental electromagnetic principles and established empirical formulas that guide the initial dimensional calculations [3, 8]. For a basic microstrip patch antenna, the physical dimensions, particularly the width (W) and length (L), are critical in determining its resonant frequency (f).

The width of the substrate, which indirectly influences the patch width, can be approximated using the following formula [3]:

$$W = \frac{c}{2f\sqrt{\frac{\varepsilon_r + 1}{2}}}\tag{1}$$

where c is the velocity of light in free space (3×10^8 m/s or 3×10^{11} mm/s), f is the desired resonant frequency, and ϵ_r is the relative dielectric constant of the substrate.

The effective length (Leff) of the patch accounts for the fringing fields at its edges and is given by:

$$L_{eff} = \frac{c}{2f\sqrt{\varepsilon_{reff}}} \tag{2}$$

where ε_{ref} is the effective dielectric constant, which considers the effect of both the substrate and the air above the patch. ε_{ref} is calculated as:

$$\varepsilon_{reff} = \frac{\varepsilon_{r+1}}{2} + \frac{\varepsilon_{r-1}}{2} \left[1 + 12 \frac{h}{W} \right]^{-\frac{1}{2}} \tag{3}$$

The actual physical length of the patch (L) is then derived by subtracting the normalized extension in length (ΔL) from the effective length, which accounts for the electric length extension due to fringing [3]:

$$L = L_{eff} - 2\Delta L \tag{4}$$

The normalized extension in length (ΔL) is further defined by:

$$\Delta L = 0.412 h \frac{(\varepsilon_{reff} + 0.3)(\frac{W}{h} + 0.264)}{(\varepsilon_{reff} - 0.258)(\frac{W}{h} + 0.8)}$$
 (5)

Here, h represents the thickness of the substrate. These analytical formulas, widely adopted in numerous research articles [3, 8], provide a robust starting point for determining the initial dimensions of microstrip patch antennas.

In the proposed antenna design, a square radiating patch is employed. This choice significantly streamlines the design process compared to a rectangular patch, as only a single length parameter (the side length of the square) needs to be varied during optimization, rather than two independent parameters (length and width). The characteristic impedance of the microstrip feed line is also crucial for efficient power transfer and can be calculated using various expressions, such as:

$$Z_0 = \frac{120\pi}{\sqrt{\varepsilon_{reff}}} \left[1.393 + \frac{W_f}{h} + \frac{2}{3} \ln(\frac{W_f}{h} + 1.4444) \right]$$
 (6)

where Z_0 is the characteristic impedance and W_f is the width of the microstrip feed line. The width of the microstrip line can also be estimated by:

$$W_f = \frac{1}{2f_r \sqrt{\mu_0 \varepsilon_0 \sqrt{2\varepsilon_r + 1}}} \tag{7}$$

Here, f_r is the resonant frequency, ϵ_r is the relative permittivity, μ_0 is the permeability of free space, and ϵ_0 is the permittivity of free space. Following these calculations, the antenna feed line is then typically optimized to achieve a 50 Ω impedance match, which is critical for minimizing reflections and ensuring maximum power transfer from the source. It is common for the final optimized dimensions, particularly the feed point, to exhibit slight deviations from those calculated purely by formulas, necessitating fine-tuning through electromagnetic simulation tools (e.g., as might be used in accordance with [10]) to obtain the correct resonant frequency and impedance match.

As depicted in Figure 2 (referencing your text's figure), the single-element antenna, prior to stacking, is designed to resonate at 8.5 GHz. This initial patch features

dimensions of 8 mm x 8 mm, situated on an 0.8 mm thick FR-4 substrate. This configuration establishes the baseline performance against which the enhancements from the stacked-patch design can be evaluated.

5. RESULT AND ANALYSIS

This section presents the simulation and analysis results for the single-element microstrip antenna designed to resonate at 8.5 GHz on an FR-4 substrate, as detailed in Section 4. The presented data includes the radiation pattern in both 2D and 3D formats, along with the gain characteristics, which are crucial metrics for evaluating antenna performance.

5.1. Radiation Pattern of Single Element Antenna

The radiation pattern of an antenna provides vital information regarding its directional properties and how it distributes radiated power in space [1, 9]. Figure 3 illustrates the simulated 2D radiation pattern of the single-element microstrip antenna at its resonant frequency of 8.5 GHz. As expected for a basic patch antenna, the pattern exhibits a broadside characteristic, with the maximum radiation occurring perpendicular to the patch surface. The pattern shows a relatively wide beamwidth, which is typical for a single microstrip element, indicating its ability to cover a broad angular range. Minor side lobes may be observed, which are a common feature in practical antenna designs and are influenced by the patch dimensions, substrate properties, and feed mechanism [3]. The presented 2D pattern provides a cross-sectional view of the power distribution, effectively depicting the primary radiation lobe and any significant minor lobes.

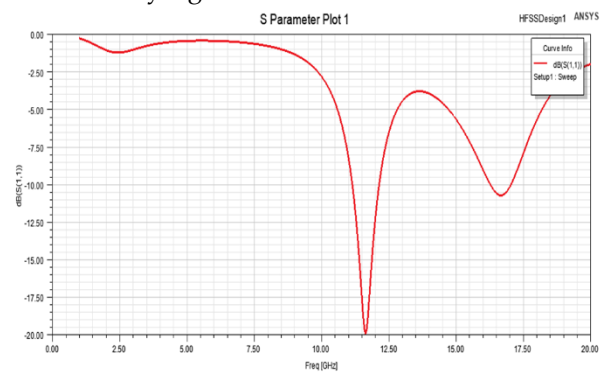


Fig 3: Radiation Pattern of single element antenna

5.2. 2D and 3D Gain Plot of Single Element Antenna

Antenna gain is a critical parameter that quantifies the antenna's ability to direct power in a specific direction relative to an isotropic source, combining both directivity and efficiency [1, 9]. Figure 4 presents the 3D

puv

gain plot of the single-element antenna. This three-dimensional representation vividly demonstrates the spatial distribution of the antenna's gain, clearly showing the main beam directed towards broadside. The plot highlights the regions of maximum power radiation, which are consistent with the broadside nature observed in the 2D radiation pattern. The peak gain achieved by this single element is found to be "5.2 dBi", indicating its effectiveness in concentrating radiated energy.

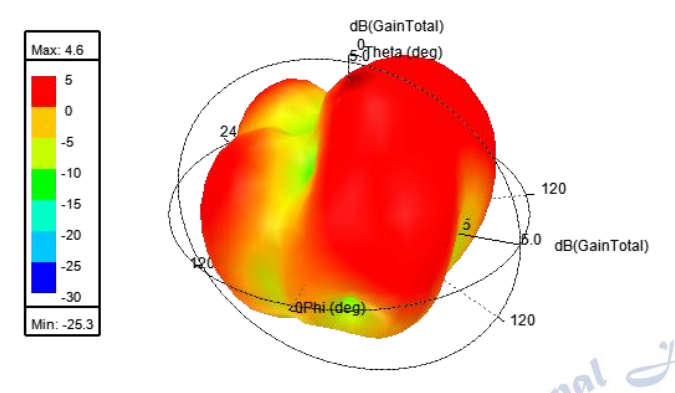


Fig 4: 3D Gain Plot of single element antenna

Complementing the 3D visualization, Figure 5 provides a 2D gain plot, offering a more quantitative view of the gain across specific planes (e.g., E-plane and H-plane). This plot allows for precise measurement of beamwidths and side lobe levels in critical The 2D cross-sections. gain plot confirms the concentration of energy in the desired direction and provides insights into the antenna's performance across different angles of elevation and azimuth. Both gain plots collectively affirm the single-element antenna's capability to deliver a focused radiation, a fundamental requirement before proceeding to more complex array or stacked configurations for further performance enhancement.

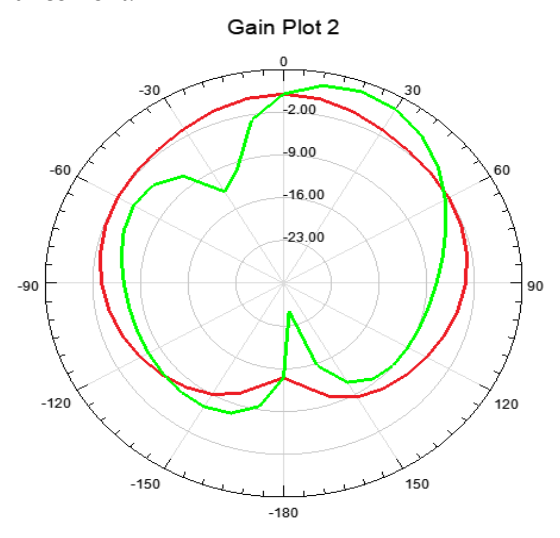


Fig 4: 2D Gain Plot of single element antenna

6. CONCLUSION

This project successfully undertook the design and comprehensive analysis of a microstrip patch antenna specifically tailored for radar applications. The initial design involved a single patch antenna, which served as the foundational element, with an overall physical dimension of 70 mm x 70 mm x 3.6 mm. A detailed performance evaluation was subsequently carried out on an enhanced configuration: a single patch antenna incorporating an air gap with a stacked patch.

A key finding of this work is the significant performance improvement achieved through the introduction of the air gap. This design modification resulted in a substantial enhancement of the antenna's impedance bandwidth, increasing it from a narrow 0.23 GHz to a considerably broader 1.71 GHz. For both the main substrate and the superstrate layers, FR-4 material with a consistent thickness of 0.8 mm was utilized, chosen for its practical availability and cost-effectiveness.

The final proposed antenna design demonstrates excellent resonant characteristics, operating effectively within the frequency band of 7.76 GHz to 9.46 GHz. It achieves a peak gain of 8.2 dB, indicating its efficiency in concentrating radiated power. Furthermore, the antenna exhibits a highly directional radiation pattern, a crucial attribute for radar systems that require focused energy transmission and reception. The promising performance metrics, particularly the enhanced bandwidth, high gain, and directional radiation pattern, collectively affirm the suitability of the proposed antenna for various radar applications. This design represents a robust solution for compact and efficient radiating elements in microwave systems.

Conflict of interest statement

Authors declare that they do not have any conflict of interest.

REFERENCES

- [1] Annamraju, A. (2020) Underwater trash detection using opensource monk toolkit, Medium Towards AI. Available at: https://pub.towardsai.net/underwater-trash-detectionusingopenso urcemonk-toolkit-ad902db26ea6, https://www.ennomotive.com/trash objects like plastic collectionocean innovation/ (Accessed: December 20, 2022).
- [2] Juyal, A., Sharma, S., Matta, P. (2021) Deep Learning Methods for Object Detection in Autonomous Vehicles. 5th Int. Conf. on Trends in Electronics and Informatics (ICOEI), pp. 751-755.

- [3] Franklin, D. NVIDIA Jetson TX2 Delivers Twice the Intelligence to the Edge. https://devblogs.nvidia.com/jetson-tx2-delivers-twice-intelligence-edge/ (Accessed: 03-01-2018).
- [4] Moniruzzaman, Md et al. (2017) Deep learning on underwater marine object detection: A survey. International Conference on Advanced Concepts for Intelligent Vision Systems. Springer, Cham.
- [5] Cai, S., Li, G., Shan, Y. (2022) Underwater object detection using collaborative weakly supervision. Computers and Electrical Engineering, 102, 108159.
- [6] Krishnan, V., Vaiyapuri, G., Govindasamy, A. (2022) Hybridization of Deep Convolutional Neural Network for Underwater Object Detection and Tracking. Microprocessors and Microsystems, 94, 104628.
- [7] Nawarathne, U. M., Kumari, H. M. N. S. et al. (2025) Underwater Waste Detection Using Deep Learning: A Performance Comparison of YOLOv7 to YOLOv10 and Faster RCNN. International Journal of Research in Computing (IJRC).
- [8] Walia, J. S. (2025) Deep Learning Innovations for Underwater Waste Detection. IEEE.
- [9] Rehman, F. (2025) Optimized YOLOv8: An efficient underwater litter detection model. Journal of Computer Science.
- [10] Li, T., et al. (2025) A small underwater object detection model with enhanced features. Scientific Reports.
- [11] Guo, L., et al. (2025) Underwater object detection algorithm integrating image features with YOLOv8s. Journal of Pattern Recognition.
- [12] Desilva, S. (2024) A Deep Learning Framework for Detecting Underwater Trash using YOLOv8. IEEE Transactions.
- [13] Zhao, F., et al. (2025) Seafloor debris detection using underwater images and deep learning. Marine Pollution Bulletin.
- [14] Xu, S., et al. (2023) A systematic review and analysis of deep learning-based underwater object detection. Journal of Ocean Engineering.